IJRCS

International Journal of Robotics and Control Systems
Vol. 3, No. 4, 2023, pp. 643-657
ISSN 2775-2658
http://pubs2.ascee.org/index.php/ijrcs

ASCEE

Comparative Study of Takagi-Sugeno-Kang and Madani Algorithms in Type-1 and Interval Type-2 Fuzzy Control for Self-Balancing Wheelchairs

Manutsawee Kiew-ong-art [a,1], Phichitphon Chotikunnan [a,2*], Anantasak Wongkamhang [a,3], Rawiphon Chotikunnan [a,4], Anuchit Nirapai [a,5], Pariwat Imura [a,6], Manas Sangworasil [a,7], Nuntachai Thongpance [a,8], Anuchart Srisiriwat [b,9]

[a] College of Biomedical Engineering, Rangsit University, Pathum Thani 12000, Thailand
[b] Department of Electrical Engineering, Pathumwan Institute of Technology, Bangkok 10330, Thailand
[1] manutsawee.s62@rsu.ac.th; [2] phichitphon.c@rsu.ac.th; [3] anantasak.w@rsu.ac.th; [4] rawiphon.c@rsu.ac.th; [5] anuchit.n@rsu.ac.th; [6] pariwat.i@rsu.ac.th; [7] manas.s@rsu.ac.th; [8] nuntachai.t@rsu.ac.th; [9] anuchart@pit.ac.th
* Corresponding Author

ARTICLE INFO

Article history
Received August 07, 2023
Revised September 17, 2023
Accepted September 22, 2023

Keywords
Fuzzy Logic;
Interval Type-2;
Self-Balancing;
Wheelchairs

ABSTRACT

This study examines the effectiveness of four different fuzzy logic controllers in self-balancing wheelchairs. The controllers under consideration are Type-1 Takagi-Sugeno-Kang (TSK) FLC, Interval Type-2 TSK FLC, Type-1 Mamdani FLC, and Interval Type-2 Mamdani FLC. A MATLAB-based simulation environment serves for the evaluation, focusing on key performance indicators like percentage overshoot, rise time, settling time, and displacement. Two testing methodologies were designed to simulate both ideal conditions and real-world hardware limitations. The simulations reveal distinct advantages for each controller type. For example, Type-1 TSK excels in minimizing overshoot but requires higher force. Interval Type-2 TSK shows the quickest settling times but needs the most force. Type-1 Mamdani has the fastest rise time with the lowest force requirement but experiences a higher percentage of overshoot. Interval Type-2 Mamdani offers balanced performance across all metrics. When a 2.7 N control input cap is imposed, Type-2 controllers prove notably more efficient in minimizing overshoot. These results offer valuable insights for future design and real-world application of self-balancing wheelchairs. Further studies are recommended for the empirical testing and refinement of these controllers, especially since the initial findings were limited to four-wheeled self-balancing robotic wheelchairs.

1. Introduction

The domain of control systems has long been a cornerstone of engineering, dating to the application of Lagrangian mechanics and Newtonian mechanics to derive the governing equations of various systems [1]-[3]. While these classical mechanics have paved the way for modern control strategies, such as Proportional-Integral-Derivative (PID) controllers, linear quadratic regulators (LQR), fuzzy logic, and neural networks, a shift toward more advanced approaches is evident [4]-[17]. Each of these control strategies offers unique advantages and limitations, particularly in applications requiring self-balancing mechanisms like wheelchairs, robots, and drones.

Despite extensive research on the performance of modern controllers, the literature lacks a comprehensive comparison of Type-1 and interval Type-2 fuzzy logic systems in different operational environments [10]-[15]. This study aims to fill this significant gap by examining the effectiveness of four different fuzzy logic controllers in self-balancing wheelchairs, namely Type-1 TSK FLS, interval Type-2 TSK FLS, Type-1 Mamdani FLS, and interval Type-2 Mamdani FLS [18]-[22]. Two testing methodologies have been designed to simulate both ideal conditions and real-world hardware limitations, and a MATLAB-based simulation environment serves for the evaluation. Key performance indicators such as percentage overshoot, rise time to a 5-second threshold, settling time, and displacement are considered [23]-[25]. It is also crucial to understand the distinguishing elements between Type-1 and interval Type-2 fuzzy logic systems. In Type-2 systems, the inclusion of a Footprint of Uncertainty (FOU) layer offers additional flexibility and nuance in control strategies [26], [27]. These controllers perform distinctly under both standard and noisy conditions, thereby adding to the broader goal of enhancing system equilibrium [28].

This research entails the development of a control system that has undergone experimental testing in real-world wheelchair systems, utilizing the TSK fuzzy logic estimation method [27]. The study specifically delves into fuzzy control systems, employing the Mamdani method [28] for estimation. Significantly, the findings of this research hold direct relevance to real-world self-balancing systems, including wheelchairs, robots, and drones. The research contributions of this study encompass a comparative evaluation of Type-1 and Type-2 fuzzy logic systems in self-balancing applications, along with a comprehensive analysis of how maximum control input limitations, such as a 2.7 N control input cap, impact the efficiency of self-balancing wheelchairs.

2. Method

2.1. Designing System of Wheelchair

In the design of the electric wheelchair balance system, a structural model of an electric wheelchair based on prior research [29] was utilized. This model was adapted to include parameters and variables tailored specifically for the study. The fundamental concept underlying the balance system is rooted in the Inverted Pendulum principle within the control system architecture. Fuzzy logic control was selected as the control methodology, with a particular focus on both TSK Type-1 and Type-2 fuzzy logic controllers, as demonstrated in previous research [26]. Real-world application testing was documented in [27]. Additionally, an exploration of the behavior of the Mamdani estimation method within the fuzzy logic control system will be elaborated upon in subsequent sections.

2.2. Dynamic Model of a Two-Wheeled Wheelchair

In the dynamic model of the two-wheeled wheelchair, a three-degree-of-freedom structure is employed, driven by eight DC motors. The first four motors control the rear wheels for linear and steering motion, while the next two are responsible for elevating the front casters. The remaining two motors adjust the position of the arm robot. The parameters used in the simulations are detailed in Table 1. The transition from a seated to a standing position involves shifting from a four-wheel to a two-wheel mode. This is achieved by moving the arm robot backward, thereby shifting the center of gravity (COG) towards the rear wheels, initiating the balancing process. The four phases of COG change are depicted in Fig 1 (b)-Fig 1 (e). A mathematical model, illustrated in Fig. 1 (f), describes the upright, two-wheel position of the wheelchair, treating it as a single-link inverted pendulum. The non-linear dynamic model is derived using the Euler-Lagrange equation, assuming no wheel-ground slippage. Equation parameters are detailed in the Appendix.

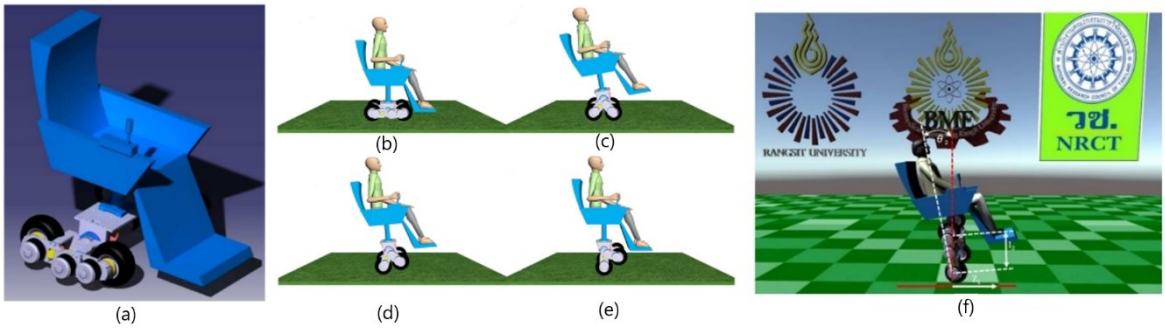

Fig. 1. The structure of the wheelchair system

Table 1. Physical parameters for simulation results

Detail	Parameter	Value	Unit
Wheel Mass	m_1	3.2000	kg
Vehicle Mass	m_2	36.1760	kg
Wheel Radius	l_1	0.1450	m
Height of the Vehicle's Center of Gravity (C.G.)	l_2	0.4025	m
Wheel Moment of Inertia	J_1	0.0250	
Vehicle Moment of Inertia	J_2	1.7363	
Gravity	g	9.8067	m/s^2

To comprehend the mechanics of the wheelchair, the system is divided into two separate components: Link 1 and Link 2, as depicted in Fig. 1 (f). Link 1 encompasses the rear wheels, while Link 2 consists of the front wheels along with the payload. The kinetic energy for Link 1 is determined using the Lagrangian function approach, as referenced in previous studies [26]-[29]. This methodology enables the computation of angular acceleration to maintain the system balance, as described in (1). Additionally, the linear acceleration while the system is in equilibrium can be derived, as indicated in (4).

$$\ddot{\theta} = \tilde{\alpha} - \tilde{\beta} \tag{1}$$

where

$$\tilde{\alpha} = \frac{\left(m_1 + m_2 + \frac{J_1}{l_1^2}\right)(m_2 l_2 g)\theta}{\left((m_2 l_2^2 + J_2)\left(m_1 + m_2 + \frac{J_1}{l_1^2}\right)\right) - (m_2 l_2)^2} \tag{2}$$

$$\tilde{\beta} = \frac{(m_2 l_2)u}{\left((m_2 l_2^2 + J_2)\left(m_1 + m_2 + \frac{J_1}{l_1^2}\right)\right) - (m_2 l_2)^2} \tag{3}$$

$$\ddot{z} = \tilde{X} - \tilde{\delta} \tag{4}$$

where

$$\tilde{X} = \frac{(m_2 l_2^2 + J_2)u}{\left((m_2 l_2^2 + J_2)\left(m_1 + m_2 + \frac{J_1}{l_1^2}\right)\right) - (m_2 l_2)^2} \tag{5}$$

$$\tilde{\delta} = \frac{(m_2^2 l_2^2 g)\theta}{\left((m_2 l_2^2 + J_2)\left(m_1 + m_2 + \frac{J_1}{l_1^2}\right)\right) - (m_2 l_2)^2} \tag{6}$$

By defining the states as $x_1 = \theta$, $x_2 = \dot{\theta}$, $x_3 = z$, and $x_4 = \dot{z}$, the corresponding state model is derived.

$$\dot{x} = Ax + bu \tag{7}$$

where

$$A = \begin{bmatrix} 0 & 1 & 0 & 0 \\ K_1 & 0 & 0 & 0 \\ 0 & 0 & 0 & 1 \\ K_3 & 0 & 0 & 0 \end{bmatrix} \tag{8}$$

$$b = \begin{bmatrix} 0 \\ K_2 \\ 0 \\ K_4 \end{bmatrix} \tag{9}$$

and the parameters are

$$K_1 = \frac{\left(m_1 + m_2 + \frac{J_1}{l_1^2}\right)(m_2 l_2 g)}{\left((m_2 l_2^2 + J_2)\left(m_1 + m_2 + \frac{J_1}{l_1^2}\right)\right) - (m_2 l_2)^2}$$

$$K_2 = \frac{-(m_2 l_2)}{\left((m_2 l_2^2 + J_2)\left(m_1 + m_2 + \frac{J_1}{l_1^2}\right)\right) - (m_2 l_2)^2}$$

$$K_3 = \frac{-(m_2^2 l_2^2 g)}{\left((m_2 l_2^2 + J_2)\left(m_1 + m_2 + \frac{J_1}{l_1^2}\right)\right) - (m_2 l_2)^2}$$

$$K_4 = \frac{(m_2 l_2^2 + J_2)}{\left((m_2 l_2^2 + J_2)\left(m_1 + m_2 + \frac{J_1}{l_1^2}\right)\right) - (m_2 l_2)^2}$$

From (8) and (9), which were initially formulated as continuous-time equations, it is possible to transition to discrete-time equations under specific conditions. This transition facilitates programmatic implementation. A sampling time of 1 millisecond or a sampling frequency of 1 kHz is employed for this purpose. The Zero-Order Hold technique is used to derive the subsequent state equations. The choice of a 1 kHz sampling frequency is suitable for developing control systems, especially in real-world testing [27], where the control must be executed through a microcontroller system. This requires processing data from various devices within the system, necessitating a sequencing of data processing. The 1 kHz frequency aligns well with the operational capabilities of the microcontroller system, making it a viable option for creating system equations at this frequency.

$$\dot{x} = \bar{A}x + \bar{b}u$$

$$\bar{A} = \begin{bmatrix} 1 & 0.001 & 0 & 0 \\ 0.001718 & 1 & 0 & 0 \\ -2.727\text{x}10^{-6} & -9.091\text{x}10^{-10} & 1 & 0.001 \\ -0.005455 & -2.727\text{x}10^{-6} & 0 & 1 \end{bmatrix}$$

$$\bar{b} = \begin{bmatrix} -4.113\text{x}10^{-8} \\ -8.225\,\text{x}10^{-5} \\ 2.126\text{x}10^{-8} \\ 4.251\text{x}10^{-5} \end{bmatrix}$$

2.3. Fuzzy Controller

This section explores the utilization of fuzzy logic systems to enhance the stability and maneuverability of the electric wheelchair. Fig. 2 provides a clear diagram illustrating the management of the chair's tilt angle and how it maintains balance on the two wheels when coming to a stop. Fuzzy logic controllers are intelligent devices well-suited for dealing with complex and dynamic systems. The design process involves several stages, including selecting inputs and outputs, defining simple variables, establishing rules, applying them, and finally converting ambiguous results into concrete actions. These controllers find applications in various fields such as traffic management, robotics, household appliances, climate control systems, and finance sectors. Ongoing research is also focused on evolving controller types [30]-[33], more adaptable models [34]-[39], and optimal control methods [40]-[45], particularly in the context of motors and robotic arms [46]-[49]. An example demonstrating the effectiveness of such controllers in maintaining stability can be found in the work of P. Chotikunnan et al. [28], where a ball and beam system was effectively managed.

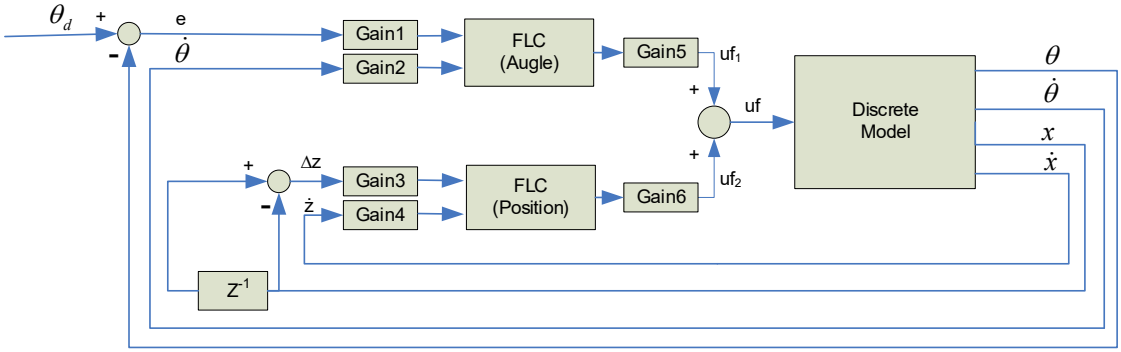

Fig. 2. Diagram depicting the control of pitch and wheel direction through the FLS method

In this study, a feedback system using fuzzy logic systems is developed to control the stability and movement of the electric wheelchair. Fig. 2 illustrates the relevant diagram. The system takes a signal, denoted as θ_d, to set the desired control angle, which in this case is fixed at 0 degrees. Two types of fuzzy logic controllers have been designed. The first controller, focusing on the angle, takes the angle error as its first input and the angular speed as its second input, producing an output named uf_1. The second controller is geared towards the position and takes the difference in displacement as its first input and linear speed as its second input, generating an output named uf_2. These outputs, uf_1 and uf_2, are then combined to form the control input signal, denoted as uf, which is fed into the system equations. Fig. 2 illustrates the role of a fuzzy logic mechanism in maintaining the balance and motion of an automated wheelchair. From the diagram, the gains, which define the range of design for any input signal, are constrained between -1 and 1. This design sets the gains of the system as follows: Gain1 is 0.0667, Gain2 is 0.05, Gain3 is 5, Gain4 is 6.6667, Gain5 is 68.67, and Gain6 is 17.1675.

In the context of the Type-1 fuzzy logic controller, a total of five distinct rules are established for the initial input, and an additional five rules are defined for the subsequent input, as visually represented in Fig. 3. Fig. 4 showcases a set of nine rules governing the output, with estimations conducted using the TSK method. Furthermore, Fig. 4 provides calculations based on the Mamdani technique, which are further elaborated upon in Table 2 and Table 3, with a specific focus on angle and positional regulation.

Turning our attention to the Type-2 fuzzy logic controller, the configuration is somewhat similar, featuring five rules for both the first and second inputs, as depicted in Fig. 5. In Fig. 6, nine rules governing the output are presented, and these rules are assessed using the TSK method. Fig. 6 also details the Mamdani method calculations, with the FOU set at 1.5. It's worth noting that increasing the FOU is an additional component that enhances the coverage and processing capabilities of the Type-2 fuzzy logic controller. Comprehensive information regarding how these fuzzy systems relate to angle and position management can be found in both Table 2 and Table 3.

Table 2. Fuzzy rules for controlling the angle

$E_\theta \setminus \dot{\theta}$	NB	NS	ZO	PS	PB
NB	PM	PB	PB	PBB	PBB
NS	PS	PM	PB	PB	PBB
ZO	NM	NS	ZO	PS	PM
PS	NBB	NS	NB	NM	NS
PB	NBB	NBB	NB	NB	NM

Table 3. Fuzzy rules for controlling the displacement

$\Delta z \setminus \dot{z}$	NB	NS	ZO	PS	PB
NB	PBB	PBB	PB	PB	PM
NS	PBB	PB	PB	PM	PS
ZO	PM	PS	ZO	NS	NM
PS	NS	NM	NB	NS	NBB
PB	NM	NB	NB	NBB	NBB

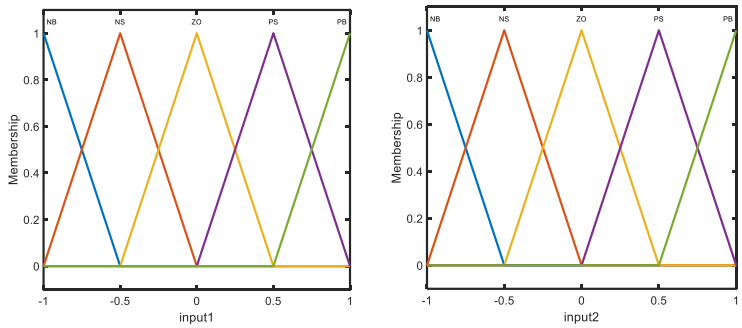

Fig. 3. Membership function of input 1 and input 2 in Type-1 fuzzy logic control

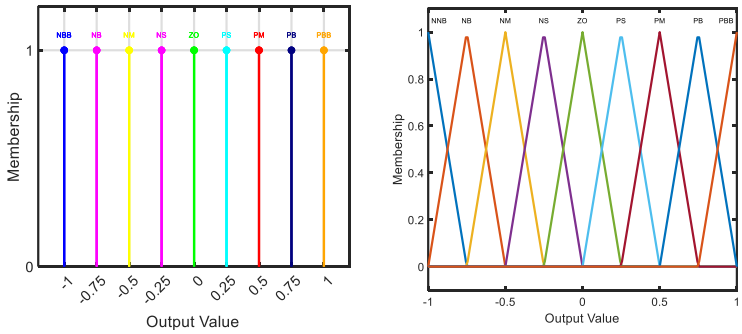

Fig. 4. Illustrates the membership function of the output in Type-1 fuzzy logic control for both TSK on the left and Mamdani on the right

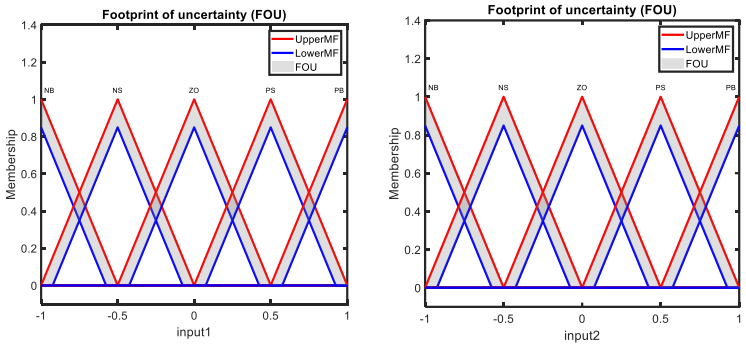

Fig. 5. Membership function of input 1 and input 2 in Type-2 fuzzy logic control

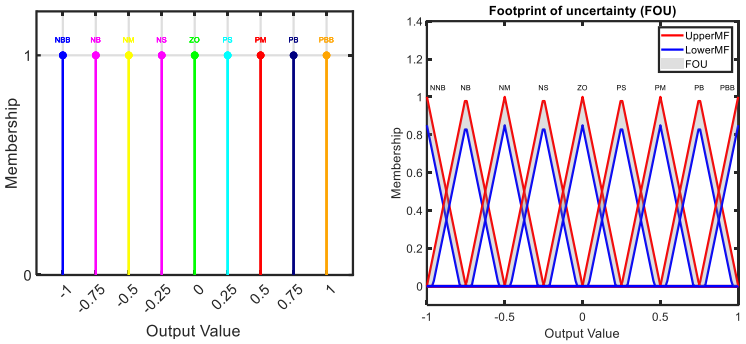

Fig. 6. Illustrates the membership function of the output in Type-2 fuzzy logic control for both TSK on the left and Mamdani on the right

In estimating the equations using the Zero-Order Type-1 TSK Fuzzy Logic System, also known as T1FLC A1C0, the value of the solution can be determined from (10). In this context, $f^i(x_i)$ represents the membership value for point x_i within the given domain of discussion.

$$y_{TSK}(x_i) = \frac{\sum_{i=1}^{M} f^i(x_i) y^i(x_i)}{\sum_{i=1}^{M} f^i(x_i)} \tag{10}$$

The Interval Type-2 fuzzy logic controller, also known as T2FLC A2C0, enhances the rule structure inherited from its Type-1 counterpart to modify its signal estimation methodology. This adaptation aims for more accurate and comprehensive signal prediction.

For generating the final crisp output value, the aggregated Type-2 fuzzy set goes through a reduction process to become an interval Type-1 fuzzy set. This set is characterized by a lower limit, denoted as y_{TSK_L}, and an upper limit, denoted as y_{TSK_R}. The final step to defuzzify the Interval Type-2 fuzzy logic controller set involves calculating the average, as indicated in (13), which is derived from the sum of (11) and (12).

$$y_{TSK\_L}(x_i) = \frac{\sum_{i=1}^{M} \underline{f^i}(x_i) y_l^i(x_i)}{\sum_{i=1}^{M} \underline{f^i}(x_i)} \tag{11}$$

$$y_{TSK\_R}(x_i) = \frac{\sum_{i=1}^{M} \overline{f^i}(x_i) y_r^i(x_i)}{\sum_{i=1}^{M} \overline{f^i}(x_i)} \tag{12}$$

$$y_{TSK\_T2}(x_i) = \frac{y_{TSK_L}(x_i) + y_{TSK\_R}(x_i)}{2} \tag{13}$$

In order to approximate the Mamdani Type I fuzzy system, (14) serves as the guideline. Here, y_{mam} stands for centroid defuzzification. This process calculates the center of gravity for the fuzzy set along the x-axis, using a formula where $\mu(x_i)$ represents the membership value of the point x_i in the specified domain.

$$y_{mam}(x_i) = \frac{\sum_i \mu(x_i)x_i}{\sum_i \mu(x_i)} \tag{14}$$

In the Type-2 Mamdani system, to derive the final crisp output value, the aggregated Type-2 fuzzy set is initially reduced to an interval Type-1 fuzzy set. This interval has a lower limit of y_{CL} and an upper limit of y_{RL}. Often referred to as the centroid of the Type-2 fuzzy set, this interval theoretically represents the average of the centroids of all embedded Type-1 fuzzy sets. However, obtaining the exact values of y_{CL} and y_{RL} isn't practically feasible. As a workaround, iterative type-reduction techniques are employed to approximate these values.

For any given aggregated Type-2 fuzzy set, (15) and (16) provide approximate values for y_{CL} and y_{RL}, respectively. These are the centroids of specific Type-1 fuzzy sets.

$$y_{CL}(x_i) = \frac{\sum_{i=1}^{L} \mu_{umf}(x_i)x_i \; + \; \sum_{i=L+1}^{N} \mu_{lmf}(x_i)x_i}{\sum_{i=1}^{L} \mu_{umf}(x_i) \; + \; \sum_{i=L+1}^{N} \mu_{lmf}(x_i)} \tag{15}$$

$$y_{RL}(x_i) = \frac{\sum_{i=1}^{R} \mu_{lmf}(x_i)x_i \; + \; \sum_{i=R+1}^{N} \mu_{umf}(x_i)x_i}{\sum_{i=1}^{R} \mu_{lmf}(x_i) \; + \; \sum_{i=R+1}^{N} \mu_{umf}(x_i)} \tag{16}$$

The interval set is converted to a crisp value using the average calculated as per (17).

$$y_{mam\_T2}(x_i) = \frac{y_{CL}(x_i) + y_{RL}(x_i)}{2} \tag{17}$$

In these equations, N represents the total number of samples collected across the output variable's range, while x_i stands for a specific sample of the output value. The upper membership function is indicated by μ_{umf}, and the lower membership function is represented by μ_{lmf}. The switch points, CL and RL, are approximated through different type-reduction techniques.

3. Results and Discussion

This study aimed to assess the effectiveness of four distinct control systems: Type-1 TSK FLC (T1 FLC A1C0), Interval Type-2 TSK FLC (T1 FLC A2C0), Type-1 Mamdani FLC, and Interval Type-2 Mamdani FLC. The assessment utilized a simulation test conducted through M-File. The primary objective was to evaluate the ability of these control systems to maintain balance in a two-wheel condition. The test initiated with an initial angle of -5 degrees, introduced a random time value of 1 millisecond, and ran for a total duration of 10 seconds.

The test scenarios were divided into two parts: the first scenario involved a test run without predetermined control input limitations for the balance-maintenance cart model. In contrast, the second scenario imposed a maximum control input limit of ±2.7N for the same cart model. The ultimate goal was to examine the efficiency and behavior of each control system, employing four distinct controller designs. The ensuing sections present the findings from these tests.

3.1. Performance under Ideal Conditions

In this section, the performance of the four fuzzy logic controllers is analyzed in ideal conditions, where no control input limitations are imposed. The evaluation focuses on essential performance metrics, including percentage overshoot, rise time, settling time, and displacement. The system's response is depicted in Fig. 7, illustrating the self-balancing wheelchair's response without control

input limitations concerning angle and angle velocity. On the left, you can see the system simulation for 10 seconds, while on the right, it displays an expanded time range from 0 to 2.5 seconds. Fig. 8 shows the system response of the self-balancing wheelchair without control input limitations in terms of position and velocity. On the left, there is an illustration of the system simulation for 10 seconds, while on the right, it shows an expanded time range from 0 to 6 seconds. Additionally, Fig. 9 provides insight into the estimated control input of the self-balancing wheelchairs without control input limitations. On the left, there is an illustration of the system simulation for 10 seconds, while on the right, it shows an expanded time range from 0 to 2 seconds.

The results and implications of this analysis can be summarized as follows: Type-1 TSK FLC excels in minimizing overshoot with only 0.7512 degrees of %OS. Its ability to maintain angles close to the setpoint makes it suitable for tasks requiring precise angle control. However, it demands a relatively high maximum force input of 34.3350 N. Interval Type-2 TSK FLC exhibits the quickest settling time, at just 2.32 seconds. However, this efficiency comes at the cost of requiring the highest force input, measuring 49.9697 N. Furthermore, it results in the least displacement, measuring 0.1092 meters.

For Type-1 Mamdani FLC, it excels in achieving the fastest rise time, registering at 0.538 seconds, and has the lowest force requirement, at 31.6704 N. However, it does exhibit a higher percentage of overshoot at 0.8064 degrees and displays the greatest displacement among all controllers, recorded at 0.2766 meters. Interval Type-2 Mamdani FLC offers balanced performance, boasting a rise time of 0.563 seconds and a settling time of 2.936 seconds. It requires a moderate force input of 33.1430 N and maintains a %OS of 1.0712 degrees. Its displacement measures 0.1748 meters, positioning it in a middle-range performance compared to the other controllers.

These findings highlight the strengths and weaknesses of each controller type under ideal conditions. Type-1 Fuzzy Systems excel at maintaining angles close to the desired setpoint, while Type-2 Fuzzy Systems exhibit greater efficiency in terms of requiring less displacement for balancing, albeit at the cost of higher force requirements. These insights are invaluable for selecting the most appropriate controller based on specific application requirements and environmental conditions. A summary of all experimental results can be found in Table 4.

Table 4. Summary of control performance in simulated tests with an initial angle of -5 degrees without control input limitations

$Initial\ angle(deg)$	Rise time (sec)	Settling time (sec)	%OS (degree)	Maximum Force(N)	Displacement (m)
T1 FLC A1C0	0.542	3.067	0.7512	34.3350	0.1933
T2 FLC A2C0	0.616	2.320	1.3227	49.9697	0.1092
T1 FLC Mamdani	0.538	3.311	0.8064	31.6704	0.2766
T2 FLC Mamdani	0.563	2.936	1.0712	33.1430	0.1748

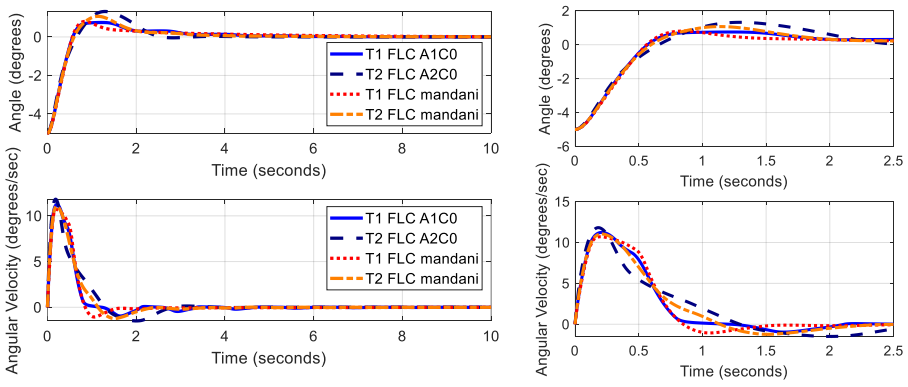

Fig. 7. System response of the self-balancing wheelchair without control input limitations in terms of angle and angle velocity

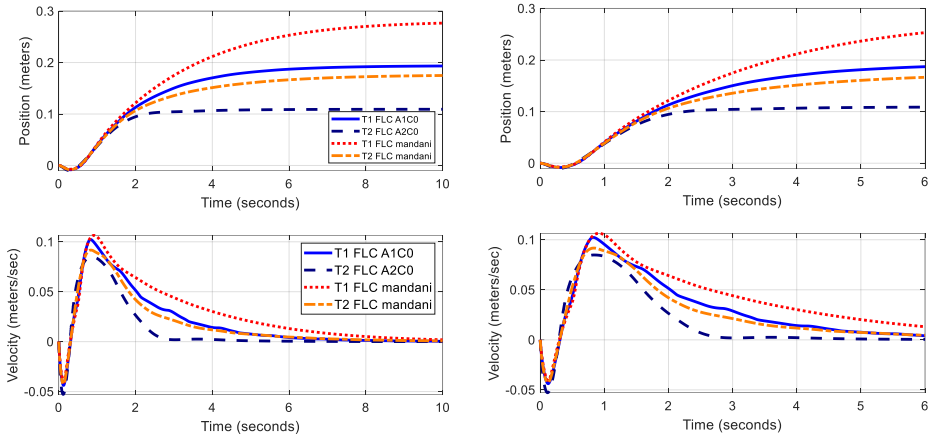

Fig. 8. System response of the self-balancing wheelchair without control input limitations in terms of position and velocity

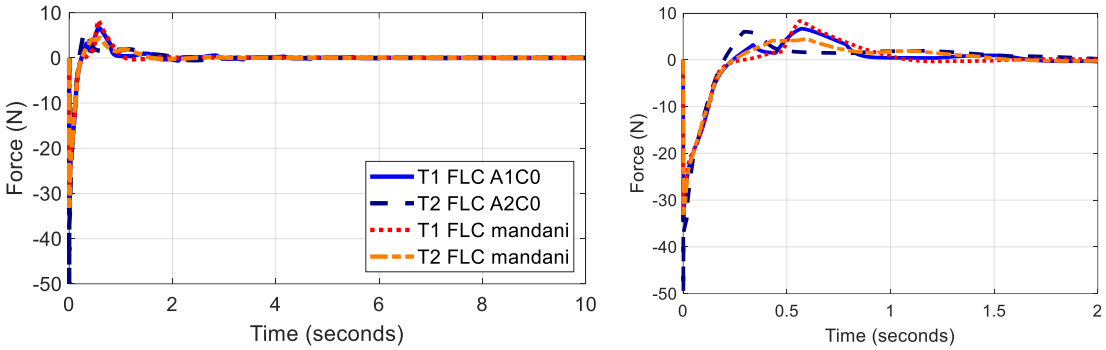

Fig. 9. Estimated control input of the self-balancing wheelchairs without control input limitations

3.2. Performance under Control Input Limitations

In this section, the performance of the fuzzy logic controller is examined under realistic constraints, where a control input cap of 2.7 N is imposed. This scenario replicates real-world hardware limitations and evaluates how well each controller adapts. The system responses are illustrated in Fig. 10, showing the self-balancing wheelchair's response to a control input limit of 2.7 N in terms of angle and angle velocity. On the left, you can see the system simulation for 10 seconds, while the right displays an expanded time range from 0 to 6 seconds. Additionally, Fig. 11 presents the system response of the self-balancing wheelchair in terms of position and velocity, also under the 2.7 N control input limit, with similar timeframes. Lastly, Fig. 12 depicts the estimated control input of the self-balancing wheelchairs under the same control input constraint.

Remarkably, Type-2 FLCs, whether in TSK or Mamdani form, consistently exhibit lower percentage overshoot (%OS) values compared to their Type-1 counterparts. This trend suggests that Type-2 systems excel at minimizing overshoot, even though they may require a greater distance to maintain balance effectively. Type-1 FLCs, when subjected to the 2.7 N control input limit, show larger %OS values, indicating their challenge in effectively controlling overshoot. However, they do manage to adapt to this control input limit, impacting certain aspects of self-balancing wheelchairs. Type-2 FLCs demonstrate their efficiency in minimizing overshoot even under control input constraints. Furthermore, they are notably more energy-efficient than Type-1 systems. Overall, these experiments' results are summarized in Table 5.

Table 5. Summary of control performance in simulated tests with an initial angle of -5 degrees with control input limit 2.7 N

Initial angle(deg)	Rise time (sec)	Settling time (sec)	%OS (degree)	Maximum Force(N)	Displacement (m)
T1 FLC A1C0	1.347	4.708	3.1136	2.7000	0.8062
T2 FLC A2C0	1.377	4.726	2.0571	2.7000	0.8742
T1 FLC Mamdani	1.346	3.847	3.5340	2.7000	0.6917
T2 FLC Mamdani	1.351	5.564	2.4981	2.7000	0.9186

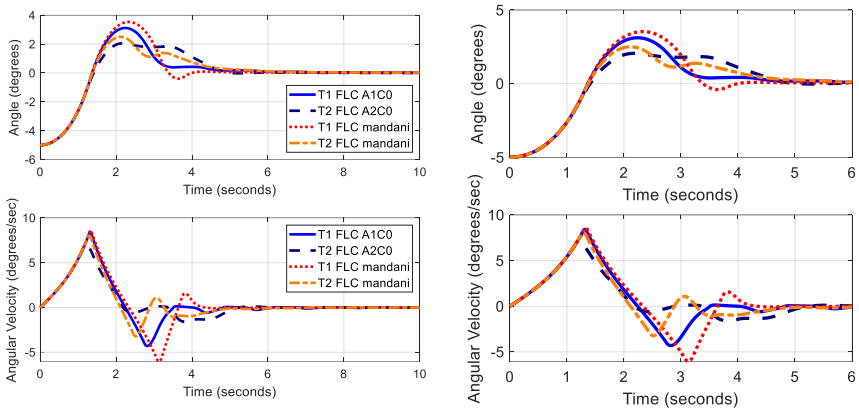

Fig. 10. System response of the self-balancing wheelchairs with control input limit 2.7 N in terms of angle and angle velocity

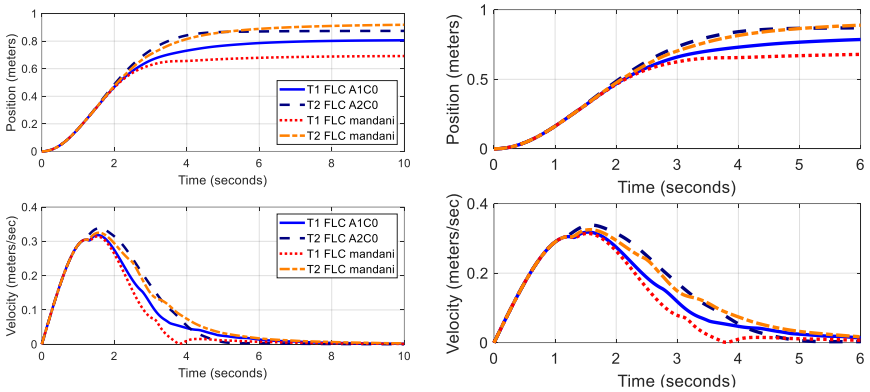

Fig. 11. System response of the self-balancing wheelchairs with control input limit 2.7 N in terms of position and velocity

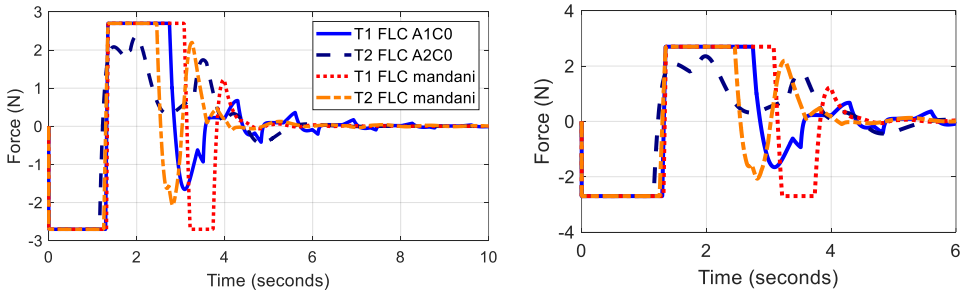

Fig. 12. Estimated control input of the self-balancing wheelchairs with control input limit 2.7 N

3.3. Conclusion and Implications

In conclusion, the results of this study provide valuable insights into the performance of different fuzzy logic controllers in self-balancing wheelchairs, both under ideal conditions and real-world

hardware limitations. These findings have significant implications for the design and application of self-balancing wheelchairs in various contexts. For future work, empirical testing and further refinement of these controllers are recommended, especially considering the initial focus on four-wheeled self-balancing robotic wheelchairs. Exploring additional real-world scenarios and applications can contribute to optimizing the choice of controller and enhancing the practicality of self-balancing wheelchairs for individuals with mobility challenges.

4. Conclusion

In conclusion, this study evaluated four distinct types of fuzzy logic controllers for self-balancing wheelchairs, including Type-1 TSK, Interval Type-2 TSK, Type-1 Mamdani, and Interval Type-2 Mamdani. The evaluation revealed significant differences in controller performance under various test conditions. Under ideal conditions, Type-1 controllers excelled at minimizing percentage overshoot (%OS) but required higher force inputs, while Type-2 controllers demonstrated faster settling times and less displacement at the expense of higher force requirements. When subjected to a 2.7 N Control Input limit, Type-1 controllers exhibited larger %OS values but adapted to the limitation. Type-2 controllers continued to minimize overshoot effectively and showed higher energy efficiency. These findings provide practical insights, with Type-1 controllers being suitable when precise control is crucial but possibly requiring higher force inputs. Type-2 controllers excel in minimizing overshoot and conserving energy, making them preferable for energy-efficient applications. This study contributes to self-balancing wheelchair technology and control system design, aiding in informed controller selection for various scenarios. Further research, including empirical testing and hybrid controller exploration, can enhance our understanding of this field.

Author Contribution: All authors contributed equally to this paper. They jointly contributed to the research and preparation of this manuscript. All authors have read and approved the final version of the paper.

Funding: This research was supported by the National Research Council of Thailand (NRCT), Research Institute, Academic Services Center, and College of Biomedical Engineering at Rangsit University.

Acknowledgment: The researchers would like to express their gratitude to the National Research Council of Thailand (NRCT), Research Institute, Academic Services Center, and College of Biomedical Engineering at Rangsit University for providing research funding to support this study.

Conflicts of Interest: The authors declare that they have no conflicts of interest to disclose.

References

[1] V. B. V. Nghia, T. Van Thien, N. N. Son, and M. T. Long, "Adaptive neural sliding mode control for two wheel self balancing robot," *International Journal of Dynamics and Control,* vol. 10, no. 3, pp. 771–784, 2022, https://doi.org/10.1007/s40435-021-00832-1.

[2] A. Mehrvarz, M. J. Khodaei, W. Clark, and N. Jalili, "A new dynamic model of a two-wheeled two-flexible-beam inverted pendulum robot," *in ASME International Mechanical Engineering Congress and Exposition*, vol. 84553, p. V07BT07A044, 2020, https://doi.org/10.1115/IMECE2020-24078.

[3] G. M. Moatimid, A. T. El-Sayed, and H. F. Salman, "Dynamical analysis of an inverted pendulum with positive position feedback controller approximate uniform solution," *Scientific Reports,* vol. 13, no. 1, p. 8849, 2023, https://doi.org/10.1038/s41598-023-34918-x.

[4] M. Magdy, A. El Marhomy, and M. A. Attia, "Modeling of inverted pendulum system with gravitational search algorithm optimized controller," *Ain Shams Engineering Journal,* vol. 10, no. 1, pp. 129-149, 2019, https://doi.org/10.1016/j.asej.2018.11.001.

[5] M. Rabah, A. Rohan, and S. H. Kim, "Comparison of position control of a gyroscopic inverted pendulum using PID, fuzzy logic and fuzzy PID controllers," *International Journal of Fuzzy Logic and Intelligent Systems,* vol. 18, no. 2, pp. 103–110, 2018, https://doi.org/10.5391/IJFIS.2018.18.2.103.

[6] D. Tran, N. Hoang, N. Loc, Q. Truong, and N. Nha, "A Fuzzy LQR PID Control for a Two-Legged Wheel Robot with Uncertainties and Variant Height," *Journal of Robotics and Control (JRC),* vol. 4, no. 5, pp. 612–620, 2023, https://doi.org/10.18196/jrc.v4i5.19448.

[7] I. Chawla and A. Singla, "Real-Time Stabilization Control of a Rotary Inverted Pendulum Using LQR-Based Sliding Mode Controller," *Arab J Sci Eng,* vol. 46, pp. 2589-2596, 2021, https://doi.org/10.1007/s13369-020-05161-7.

[8] S. J. Chacko and R. J. Abraham, "On LQR controller design for an inverted pendulum stabilization," *International Journal of Dynamics and Control,* vol. 11, no. 4, pp. 1584–1592, 2023, https://doi.org/10.1007/s40435-022-01079-0.

[9] B. Bekkar and K. Ferkous, "Design of Online Fuzzy Tuning LQR Controller Applied to Rotary Single Inverted Pendulum: Experimental Validation," *Arabian Journal for Science and Engineering,* vol. 48, no. 5, pp. 6957-6972, 2023, https://doi.org/10.1007/s13369-022-06921-3.

[10] K. Ashwani and N. Yadnyesh, "Control Optimization of Triple-Stage Inverted Pendulum Using PID-Based ANFIS Controllers," *in Advances in Systems Engineering: Select Proceedings of NSC 2019,* pp. 501-514, Singapore: Springer, 2021, https://doi.org/10.1007/978-981-15-8025-3_49.

[11] M. A. R. Shafei, D. K. Ibrahim, and M. Bahaa, "Application of PSO tuned fuzzy logic controller for LFC of two-area power system with redox flow battery and PV solar park," *Ain Shams Engineering Journal,* vol. 13, no. 5, p. 101710, 2022, https://doi.org/10.1016/j.asej.2022.101710.

[12] A. Ansarian and M. J. Mahmoodabadi, "Multi-objective optimal design of a fuzzy adaptive robust fractional-order PID controller for a nonlinear unmanned flying system," *Aerospace Science and Technology,* vol. 141, p. 108541, 2023, https://doi.org/10.1016/j.ast.2023.108541.

[13] M. F. Masrom, N. M. A Ghani, and M. O. Tokhi, "Particle swarm optimization and spiral dynamic algorithm-based interval type-2 fuzzy logic control of triple-link inverted pendulum system: A comparative assessment," *Journal of Low Frequency Noise, Vibration and Active Control,* vol. 40, no. 1, pp. 367-382, 2021, https://doi.org/10.1177/1461348419873780.

[14] A. A. bin Abdul Razak, A. N. K. bin Nasir, N. M. A. Ghani, S. Mohammad, M. F. M. Jusof, and N. A. M. Rizal, "Hybrid genetic manta ray foraging optimization and its application to interval type 2 fuzzy logic control of an inverted pendulum system," *in IOP Conference Series: Materials Science and Engineering,* vol. 917, no. 1, p. 012082, 2020, https://doi.org/10.1088/1757-899X/917/1/012082.

[15] J. Shi, "Structure Analysis of General Type-2 Fuzzy Controller and Its Application," *International Journal of Fuzzy System Applications (IJFSA),* vol. 12, no. 1, pp. 1–20, 2023, https://doi.org/10.4018/ijfsa.319813.

[16] I. Gandarilla, J. Montoya-Cháirez, V. Santibáñez, C. Aguilar-Avelar, and J. Moreno-Valenzuela, "Trajectory tracking control of a self-balancing robot via adaptive neural networks," *Engineering Science and Technology, an International Journal,* vol. 35, p. 101259, 2022, https://doi.org/10.1016/j.jestch.2022.101259.

[17] D. M. Nguyen, N. Van-Tiem, and T. T. Nguyen, "A neural network combined with sliding mode controller for the two-wheel self-balancing robot," *IAES International Journal of Artificial Intelligence,* vol. 10, no. 3, p. 592, 2021, https://doi.org/10.11591/ijai.v10.i3.pp592-601.

[18] I. A. Hashim, E. H. Karam, and N. S. Abdul-Jaleel, "Design and Implementation of a Two Stage Controller for Ball and Beam System Using FPGA," *Engineering and Technology Journal,* vol. 36, no. 4, pp. 381-390, 2018, https://doi.org/10.30684/etj.36.4A.4.

[19] R. Deepa, R. Velnath, E. H. Guhan, C. Moorthy, P. Gomathi, and A. Dinesh, "Stability Analysis of Ball and Beam System using PID Controller," *in 2021 International Conference on Advancements in Electrical, Electronics, Communication,* Computing and Automation (ICAECA), pp. 1-4, 2021, https://doi.org/10.1109/icaeca52838.2021.9675724.

[20] O. T. Altinoz and A. E. Yilmaz, "Investigation of the Optimal PID-Like Fuzzy Logic Controller for Ball and Beam System with Improved Quantum Particle Swarm Optimization," *International Journal of Computational Intelligence and Applications,* vol. 21, no. 04, p. 2250025, 2022, https://doi.org/10.1142/s1469026822500250.

[21] I. H. Ibrahim and H. I. Ali, "Quantitative PID Controller Design using Black Hole Optimization for Ball and Beam System," *IRAQI JOURNAL OF COMPUTERS, COMMUNICATIONS, CONTROL AND SYSTEMS ENGINEERING,* vol. 21, no. 3, pp. 65-75, 2021, https://doi.org/10.33103/uot.ijccce.21.3.6

[22] V. Srivastava and S. Srivastava, "Hybrid optimization based PID control of ball and beam system," *Journal of Intelligent & Fuzzy Systems,* vol. 42, no. 2, pp. 919-928, 2022, https://doi.org/10.3233/JIFS-189760.

[23] N. S. Abdul Aziz, N. Ishak, R. Adnan, and M. Tajjudin, "Hybrid fuzzy PID controller design for ball and beam system," *Journal of Electrical and Electronic Systems Research (JEESR),* vol. 15, pp. 47-51, 2019, https://ir.uitm.edu.my/id/eprint/48855/.

[24] X. Huang, A. L. Ralescu, H. Gao, and H. Huang, "A survey on the application of fuzzy systems for underactuated systems," *Proceedings of the Institution of Mechanical Engineers, Part I: Journal of Systems and Control Engineering,* vol. 233, no. 3, pp. 217-244, 2019, https://doi.org/10.1177/0959651818791027.

[25] M. K. Saleem, M. L. U. R. Shahid, A. Nouman, H. Zaki, and M. A. U. R. Tariq, "Design and implementation of adaptive neuro-fuzzy inference system for the control of an uncertain ball and beam apparatus," *Mehran University Research Journal of Engineering & Technology,* vol. 41, no. 2, pp. 178-184, 2022, https://doi.org/10.22581/muet1982.2202.17.

[26] B. Panomruttanarug and P. Chotikunnan, "Self-balancing iBOT-like wheelchair based on type-1 and interval type-2 fuzzy control," *in 2014 11th International Conference on Electrical Engineering/Electronics, Computer, Telecommunications and Information Technology (ECTI-CON),* pp. 1-6, 2014, https://doi.org/10.1109/ECTICon.2014.6839710.

[27] P. Chotikunnan and B. Panomruttanarug, "The application of fuzzy logic control to balance a wheelchair," *Journal of Control Engineering and Applied Informatics,* vol. 18, no. 3, pp. 41-51, 2016, http://www.ceai.srait.ro/index.php?journal=ceai&page=article&op=view&path%5B%5D=3173.

[28] R. Chotikunnan, P. Chotikunnan, A. Ma'arif, N. Thongpance, Y. Pititheeraphab, and A. Srisiriwat, "Ball and Beam Control: Evaluating Type-1 and Interval Type-2 Fuzzy Techniques with Root Locus Optimization," *International Journal of Robotics and Control Systems,* vol. 3, no. 2, pp. 286–303, 2023, https://doi.org/10.31763/ijrcs.v3i2.997.

[29] G. Vailland *et al*., "VR based Power Wheelchair Simulator: Usability Evaluation through a Clinically Validated Task with Regular Users," *2021 IEEE Virtual Reality and 3D User Interfaces (VR)*, pp. 420-427, 2021, https://doi.org/10.1109/VR50410.2021.00065.

[30] M. Rabah, A. Rohan, Y. J. Han, and S. H. Kim, "Design of fuzzy-PID controller for quadcopter trajectory-tracking," *International Journal of Fuzzy Logic and Intelligent Systems,* vol. 18, no. 3, pp. 204-213, 2018, https://doi.org/10.5391/IJFIS.2018.18.3.204.

[31] M. J. Mohamed and M. Y. Abbas, "Design of a Fuzzy PID Controller for Trajectory Tracking of a Mobile Robot," *Engineering and Technology Journal,* vol. 36, no. 1, pp. 100-110, 2018, https://doi.org/10.30684/etj.36.1A.15.

[32] K. Lee, D. Y. Im, B. Kwak, and Y. J. Ryoo, "Design of fuzzy-PID controller for path tracking of mobile robot with differential drive," *International Journal of Fuzzy Logic and Intelligent Systems,* vol. 18, no. 3, pp. 220-228, 2018, https://doi.org/10.5391/IJFIS.2018.18.3.220.

[33] K. Eltag, M. S. Aslamx, and R. Ullah, "Dynamic Stability enhancement using fuzzy PID control technology for power system," *International Journal of Control, Automation and Systems,* vol. 17, pp. 234-242, 2019, https://doi.org/10.1007/s12555-018-0109-7.

[34] J.Y. Zhai and Z.B. Song, "Adaptive sliding mode trajectory tracking control for wheeled mobile robots," *International Journal of Control,* vol. 92, no. 10, pp. 2255-2262, 2019, https://doi.org/10.1080/00207179.2018.1436194.

[35] L. Gracia, J.E. Solanes, P. Muñoz-Benavent, J.V. Miro, C. Perez-Vidal, and J. Tornero, "Adaptive sliding mode control for robotic surface treatment using force feedback," *Mechatronics,* vol. 52, pp. 102-118, 2018, https://doi.org/10.1016/j.mechatronics.2018.04.008.

[36] T. Zhang, Y. Yu, and Y. Zou, "An adaptive sliding-mode iterative constant-force control method for robotic belt grinding based on a one-dimensional force sensor," *Sensors,* vol. 19, no. 7, p. 1635, 2019, https://doi.org/10.3390/s19071635.

[37] B. Jiang, H.R. Karimi, S. Yang, C. Gao, and Y. Kao, "Observer-based adaptive sliding mode control for nonlinear stochastic Markov jump systems via T–S fuzzy modeling: Applications to robot arm model," *IEEE Transactions on Industrial Electronics,* vol. 68, no. 1, pp. 466-477, 2020, https://doi.org/10.1109/tie.2020.2965501.

[38] K. Liu, H. Gao, H. Ji, and Z. Hao, "Adaptive sliding mode based disturbance attenuation tracking control for wheeled mobile robots," *International Journal of Control, Automation and Systems,* vol. 18, no. 5, pp. 1288-1298, 2020, https://doi.org/10.1007/s12555-019-0262-7.

[39] F. Ejaz, M.T. Hamayun, S. Hussain, S. Ijaz, S. Yang, N. Shehzad, and A. Rashid, "An adaptive sliding mode actuator fault tolerant control scheme for octorotor system," *International Journal of Advanced Robotic Systems, vol*. 16, no. 2, 2019, https://doi.org/10.1177/1729881419832435.

[40] C. Sánchez-Sánchez and D. Izzo, "Real-time optimal control via deep neural networks: study on landing problems," *Journal of Guidance, Control, and Dynamics,* vol. 41, no. 5, pp. 1122-1135, 2018, https://doi.org/10.48550/arxiv.1610.08668.

[41] N. Razmjooy and M. Ramezani, "Optimal control of two-wheeled self-balancing robot with interval uncertainties using Chebyshev inclusion method," *Majlesi Journal of Electrical Engineering,* vol. 12, no. 1, pp. 13-21, 2018, https://doi.org/10.1002/asjc.1777.

[42] X. Long, Z. He, and Z. Wang, "Online optimal control of robotic systems with single critic NN-based reinforcement learning," *Complexity,* 2021, https://doi.org/10.1155/2021/8839391

[43] Y. Pan, C. A. Cheng, K. Saigol, K. Lee, X. Yan, E. A. Theodorou, and B. Boots, "Imitation learning for agile autonomous driving," *The International Journal of Robotics Research,* vol. 39, no. 2-3, pp. 286-302, 2020, https://doi.org/10.1177/0278364919884027.

[44] C. L. Dembia, N. A. Bianco, A. Falisse, J. L. Hicks, and S. L. Delp, "Opensim moco: Musculoskeletal optimal control," *PLOS Computational Biology,* vol. 16, no. 12, p. e1008493, 2020, https://doi.org/10.1371/journal.pcbi.1008493.

[45] B. Zhao, D. Liu, and C. Luo, "Reinforcement learning-based optimal stabilization for unknown nonlinear systems subject to inputs with uncertain constraints," *IEEE Transactions on Neural Networks and Learning Systems,* vol. 31, no. 10, pp. 4330-4340, 2019, https://doi.org/10.1109/tnnls.2019.2954983.

[46] N. Singh, A. K. Sharma, M. Tiwari, M. Jasiński, Z. Leonowicz, S. Rusek, and R. Gono, "Robust Control of SEDCM by Fuzzy-PSO," *Electronics,* vol. 12, no. 2, pp. 335, 2023, https://doi.org/10.3390/electronics12020335.

[47] Ö. Bingül and A. Yıldız, "Fuzzy Logic and Proportional Integral Derivative Based Multi-Objective Optimization of Active Suspension System of a 4 × 4 In-Wheel Motor Driven Electrical Vehicle," *J. Vibration and Control,* vol. 29, no. 5-6, pp. 1366-1386, Mar. 2023, https://doi.org/10.1177/10775463211062691.

[48] D. Saputra, A. Ma'arif, H. Maghfiroh, P. Chotikunnan, and S. Rahmadhia, "Design and Application of PLC-based Speed Control for DC Motor Using PID with Identification System and MATLAB Tuner," *Int. J. Robotics and Control Systems,* vol. 3, no. 2, pp. 233-244, 2023, https://doi.org/10.31763/ijrcs.v3i2.775

[49] H. Huang, H. Xu, F. Chen, C. Zhang, and A. Mohammadzadeh, "An Applied Type-3 Fuzzy Logic System: Practical Matlab Simulink and M-Files for Robotic, Control, and Modeling Applications," *Symmetry,* vol. 15, no. 2, pp. 475, 2023, https://doi.org/10.3390/sym15020475.